Research article
doi.org/10.1002/elsa.202100021
Chemistry Europe
European Chemical Societies Publishing

Received: 3 February 2021
Revised: 8 April 2021
Accepted: 16 April 2021

Properties of electrochemically copolymerized aniline and melamine on functionalized multiwalled-carbon nanotube film electrodes

Guo Xiong Tham[1,2] | **Arnold Subrata**[1] | **Adrian C. Fisher**[2,3] | **Richard D. Webster**[1,2]

[1] Division of Chemistry and Biological Chemistry, School of Physical and Mathematical Sciences, Nanyang Technological University, Singapore, Singapore

[2] Cambridge Centre for Advanced Research and Education in Singapore, Singapore, Singapore

[3] Department of Chemical Engineering and Biotechnology, University of Cambridge, Cambridge, UK

Correspondence
Richard D. Webster, Division of Chemistry and Biological Chemistry, School of Physical and Mathematical Sciences, Nanyang Technological University, 21 Nanyang Link, Singapore 637371, Singapore.
Email: webster@ntu.edu.sg

Funding information
the National Research Foundation (NRF) Singapore under its Campus for Research Excellence and Technological Enterprise (CREATE) program; the Singapore Government MOE Academic Research Fund Tier 1, Grant/Award Number: RG3/19

Abstract

The electrochemical properties of polymerized aniline (PANI) and polymerized melamine (PMEL) that were electrochemical copolymerized (PANIMEL) on a glassy carbon electrode (GCE) that had been coated with functionalized multiwalled carbon nanotubes (fMWCNT) to form a PANIMEL/fMWCNT/GCE film electrode were studied, with an aim toward electrochemical energy storage (EES). A number of factors, such as the choice of working electrode, electrolyte, switching potential, applied scan rate, and type of fMWCNTs, were initially investigated and evaluated during the individual electrochemical polymerization of aniline and melamine via successive potential cycling. The electrochemical copolymerisation of aniline and melamine was then studied with an ideal monomeric ratio of 1:3 that gave an optimal ratio of the voltammetric peak current heights with distinguishable redox peak potentials. Variable scan rate cyclic voltammetry (CV) of the electrosynthesized copolymer film electrode confirmed the dominance of the surface-confined electron transfer process at the electrode. The electrochemical stability of the copolymer film electrode was also assessed and revealed a limited cyclability of the daughter polymeric melamine, which was hypothesized to be due to an excessive nitrogen content combined with a low porosity that led to a poor ion intercalation-deintercalation mechanism. Electrochemical impedance spectroscopy (EIS) was performed to evaluate the electrochemical performance of the copolymerized film electrode with other control electrodes. The corresponding EIS results suggested that the copolymerized film electrode was electrochemically superior to the PMEL/fMWCNT/GCE film electrode but was inferior to the PANI/fMWCNT/GCE film electrode.

KEYWORDS
aniline, carbon nanotubes, copolymerization, electrochemical energy storage, melamine

Research article
doi.org/10.1002/elsa.202100021
Chemistry Europe
European Chemical Societies Publishing

1 | INTRODUCTION

Rapid economic growth has led to an ever-increasing demand for energy in the 21st century. In the present day, electrical energy is primarily obtained from the burning of fossil fuels, such as oil, coal, and natural gas, to power homes and industries. Countries around the world have been exploring alternative energy sources that are sustainable, pollution free, easy to reproduce, and economically affordable to generate electricity and drive the green economy while meeting the global energy demand of an ever-increasing world population. The development and use of nanotechnology by scientists from various disciplines for energy storage applications is part of this green economy.[1] An alternative solution to efficient energy storage is the use of supercapacitors, which are electrochemical energy storage (EES) devices. Supercapacitors store large quantities of energy with high power, high cyclability, and are environmental friendly. Generally, EES involves current (electron) flow between two conducting electrodes separated by an ionic medium (electrolyte) to facilitate the occurrence of redox chemical reactions at the surfaces of both electrodes. Reduction and oxidation reactions occur at the cathode and anode, respectively.[2]

In the field of EES, carbon nanotubes (CNTs) display a promising potential for their use owing to their excellent electrical conductivity, high surface areas, and increased pore accessibility. However, the energy density of CNTs can be further enhanced by the combination of CNTs and conducting polymers (CPs) that are commonly used to fabricate composites ranging from micro- to nanosize in thickness. The specific capacitance of purified CNTs lies in the range of 20–80 F/g and is enhanced if interactions occur with a pseudocapacitive material such as CPs.[3] For instance, the polyaniline-CNT (PANI-CNT) composite electrode had a greater specific capacitance than its sole PANI electrode, which makes the former commonly used as electrode materials for supercapacitors.[4] The use of CNTs can also overcome the limitation of cyclability lifetime associated with several CPs that experience swelling and shrinking during charging/discharging processes. Moreover, electrically conductive CNTs help to decrease polymer resistance and enhance the porosity and specific surface area of the polymer-CNT composites for charge transport. With such excellent inherent characteristics, CNTs and CPs are commonly and widely coused to fabricate electrodes of EES devices, including supercapacitors and lithium-ion batteries (LIBs), to enhance their power density.[5,6]

For EES devices to work well, their electrode materials should generally possess the merits of high electrical conductivity, high chemical and physical stabilities, high specific surface area, and high porosity for fast diffusion to the electrode material.[7] To date, several research studies have reported on a combination of CPs and CNTs that are used as electrode materials via various methods of synthesis. Chemical and electrochemical polymerization are more commonly used, while less common methods, such as mechanical mixing [8] and layer-by-layer assembly,[9] have been reported. Although the chemical functionalization of CNTs creates structural defects to affect the conductivity of composite electrodes, the use of electroactive materials with these CNTs can still alleviate this problem. In particular, multiwalled CNTs (MWCNTs) are usually preferred more than single-walled CNTs as the capacitance is twice as much as for the former than the latter due to the highly mesoporous structure allowing for more charge accumulation at the electrode-electrolyte interface.[10]

Numerous articles have reported the use of pristine and chemically functionalized CNTs with polymerized aniline (PANI) but with very limited reports on the use of these CNTs with polymerized melamine (PMEL) in EES applications. This report investigates the possibility of developing a PANIMEL/fMWCNT/GCE copolymerized film electrode for EES applications that incorporates melamine and aniline via an in-*situ* electrochemical copolymerization on the fMWCNT/GCE electrode surface. Melamine, aniline, and MWCNTs with carboxylic acid functionalization (fMWCNTs) were picked due to their ready commercial obtainability, low cost, and because little work to date has been carried out on such a combination. The use of fMWCNTs was more favored over their nonfunctionalized forms to reduce the tendency of agglomeration and to avoid the use of surfactants required with pristine CNTs that could cause inefficiencies in industrial processing.[11] Studies have also indicated that the composite materials that involve heteroatoms with carbons can reduce the band gap between the conduction and valence bands and thereby increase the electrical conductivity of these electrodes.[12,13] The high nitrogen contents of melamine and aniline in their polymeric forms can potentially induce strong pseudocapacitive effects in the electrochemical performance of supercapacitor electrodes. The use of acids or bases can also activate CNTs by enlarging the micropore volume of the CNTs to enhance charge storage and transport.[14] Various factors to optimize the electrochemical performance of the composite film electrode materials were investigated and evaluated accordingly. In addition, electrochemical impedance studies (EIS) were performed to offer insights into the nature and extent of the interfacial charge transfer processes occurring in various composite electrodes, and thereby, evaluate whether the copolymerized PANIMEL/fMWCNT/GCE film electrode can be potentially used in the applications of EES.

Research article
doi.org/10.1002/elsa.202100021
Chemistry Europe
European Chemical Societies Publishing

2 | MATERIALS AND METHODS

2.1 | Chemicals

Aniline (>99%) and melamine (99%) were obtained from Alfa Aesar. Potassium hexacyanoferrate(II) trihydrate (≥98.5%) and potassium hexacyanoferrate(III) (≥99.0%) were ACS reagent grade and obtained from Merck. Hydrochloric acid (37%) was obtained from VWR Chemicals. Ultrapure water with resistivity not less than 18 MΩ cm was obtained from an ELGA Purelab Option-Q water purification system. HCl solution (1.0 M) was prepared from the dilution of a stock solution with ultrapure water. MWCNTs with carboxylic acid functionalization (fMWCNTs) (95%, 50–80 nm diameter, and 10–20 μm length) were obtained from Nanostructured and Amorphous Materials Inc. in Texas, USA. Ethanol (Fisher Chemical) was reagent grade and used as received.

2.2 | Preparation of the modified electrodes

Prior to the drop casting of the fMWCNT suspension on the electrode surface, the Metrohm 3 mm planar diameter GC electrode was polished with 0.3 μm grit alumina oxide powder on the Buehler Ultra-Pad polishing cloth, rinsed thoroughly with ultrapure water to remove any residual powder and then dried clean with lint-free paper. A fMWCNT suspension was prepared by dissolving 4 mg of fMWCNT in 4 mL ethanol and subsequently ultrasonicated at room temperature (22 ± 2°C). A 10 μL aliquot of the fMWCNT dispersion was then deposited on the surface of the glassy carbon electrode (GCE) with a micropipette and the solvent then left to evaporate in the air for 5 to 10 min. The drop casting process was repeated for another two times before immersing in a solution that was contained within the electrochemical glass cell.

2.3 | Electrochemical procedures

CV and EIS experiments were performed with computer-controlled Eco Chemie Autolab PGSTAT302N and PGSTAT203N potentiostats, respectively, in a three-electrode cell. The auxiliary electrode used in all electrochemical experiments consisted of a platinum wire along with a silver chloride reference electrode (Ag/AgCl in 3 M KCl). The working electrode containing the drop cast fMWCNT suspension together with the auxiliary and reference electrodes were subsequently immersed in the solution contained in the glass cell. The electrochemical cell was fully assembled in a Faraday cage to minimize any external electromagnetic interference caused while performing the electrochemical scans. A fresh solution was prepared at each desired pH prior to the voltammetric measurement and experiments were conducted at room temperature (22 ± 2°C). CVs were recorded with a scan rate of 20 mV/ s unless otherwise stated. EIS measurements were recorded with a frequency range from 0.1 to 60 kHz.

2.4 | Characterization procedures

Scanning electron microscopy (SEM) and energy-dispersive X-ray spectroscopy were performed using a JEOL JSM-7600 Schottky field emission scanning electron microscope (Japan). X-ray photoelectron spectroscopy (XPS) was performed on an ESCAProbeP (Omicron Nanotechnology Ltd., Taunusstein, Germany) spectrometer equipped with a monochromatic Mg X-ray source (1253.6 eV). The binding energy of the C1s peak (285 eV) was used for spectral calibration.

3 | RESULTS AND DISCUSSION

3.1 | Electrochemical polymerization of individual monomers

3.1.1 | Choice of working electrode

In order to select the best working electrode for this study, the characteristics of the electrodes as supercapacitors were studied and aligned to the aims of the project. Generally, the electrodes used should be physically hard and strong, environmental friendly, highly conductive, resistant against corrosion, and have good chemical and temperature stability. A 3-mm GCE as the base material to support the composite materials was picked over inert metal surfaces, such as platinum or gold, due the lower cost of a carbon-based material, particularly if it needs to be increased in size for an industrial application.

3.1.2 | Choice of supporting electrolyte

It is well known that the certain electrolytes can enhance the specific capacitance of the electrode materials. Therefore, the choice of a supporting electrolyte is essential to contribute to the proper electrochemical performances of the electrochemical capacitor electrodes. Aqueous inorganic electrolytes have their operating voltage window significantly narrower than the organic forms and thereby can limit the energy density of the electrode materials.[15,16] Nevertheless, aqueous electrolytes are preferred over their

Research article
doi.org/10.1002/elsa.202100021
Chemistry Europe
European Chemical Societies Publishing

organic counterparts to address the goal of developing a green electrode material, as most organic electrolytes are classified as toxic and carcinogenic. Moreover, their advantages of having higher ionic conductivity and lower viscosity offer faster cycling rates of charging and discharging.[17] Low cost and simplicity of preparing aqueous electrolytes can also reduce the cost of constructing the electrodes used in EES.

Various aqueous electrolytes, such as hydrochloric acid and sulfuric acid, were explored. These aqueous electrolytes have high ionic concentration and low resistance, but hydrochloric acid was found to be best suited for the electrochemically copolymerization of aniline and melamine. In a strongly acidic medium (pH < 2.5), aniline can be electrochemically polymerized to give an electrically conductive PANI due to the doping of the emeraldine form of the polymer species with the protonic acid.[18,19] Moreover, the strong affinity of the chloride anions as dopants to PMEL enhances the polymer conductivity with the chloride anions acting as counterions to the positively charged sites of the electrosynthesized polymers.[20]

3.1.3 | Choice of applied scan rate

In most electrochemical polymerization processes, a relatively slow scan rate is required to allow a slower rate of potential change to generate more charge carriers and insert more anions (or dopants) into the polymeric backbone for charge neutrality, enhanced doping levels, and better polymer conductivity.[21] Thus, a scan rate of 20 mV/s was applied to every successive potential cycling for the electrochemical polymerization processes in this study.

3.1.4 | Choice of fMWCNTs

Aniline can be electrochemically polymerized with and without the fMWCNTs being drop cast on the bare GCE surface. On the contrary, electrochemical polymerization of melamine can only occur strongly when functionalized CNTs (fCNTs) are used.[22] The presence of the fCNTs promotes interactions with the organic polymer species and offers a pathway for charge transfer to occur across the interconnected fCNT-polymer network. To verify such a response, a bare GCE was initially used in the study for potential cycling in 1.0 M HCl solution as the supporting electrolyte with a switching potential of 1.4 V at a scan rate of 20 mV/s. Indeed, there was only very weak to no electrochemical polymerization with almost constant voltammetric peak currents at ca. 0.70 V during the successive potential cycling. However, with the use of drop cast fMWCNTs, electrochemical polymerization of melamine did occur with increasing anodic and cathodic current heights during the potential cycling, which shall be described in the following subsection on the choice of switching potential. Thus, fMWCNTs were drop cast onto a clean GCE surface prior to the all the electrochemical polymerization experiments.

3.1.5 | Choice of switching potential

Figure 1 shows the CVs of the electrochemical polymerization of 2 mM melamine on the surface of the fMWCNT/GCE film electrode at various switching potentials of 0.8, 1.0, 1.2, 1.4, 1.5, and 1.6 V versus Ag/AgCl in 1.0 M HCl with an applied scan rate of 20 mV/s for 20 successive potential cycles. In these aforementioned switching potentials, the electrochemical polymerization of melamine occurred in the potential range of 0.4 to 0.8 V. In addition, the corresponding anodic and cathodic current densities increased as the cycle number increased from 0 to 20 for any switching potential between 0.8 and 1.6 V. Moreover, the anodic and cathodic waves between 0.4 and 0.8 V were noted to shift in the positive and negative directions, respectively, with repeated scans which implied an increase in the internal resistance of the electrode due to the increased thickness of the polymerized layer caused by the electrochemical polymerization of melamine on the surface of the fMWCNT/GCE film electrode.

When the switching potential was ≤1.2 V, electrochemical polymerization of melamine was noted at an oxidative potential of 0.45 V. Upon increasing the switching potential to 1.4 V (Figure 1d), the corresponding anodic peak potential shifted positively to 0.74 V with its current density increased by approximately 56 times more than that of the switching potential at 0.8 V (Figure 1a). Thus, it can be determined that a switching potential of 1.4 V is ideal for the electrochemical polymerization of melamine to occur.

While comparing the CVs at switching potentials of 1.4, 1.5, and 1.6 V (Figure 1d to f), three observations can be made. First, the anodic peak currents of the final (20th) potential cycle at a switching potential of 1.6 V (Figure 1f) was smaller than that at 1.4 and 1.5 V (Figure 1d and e). A diminishing peak current at a switching potential of 1.6 V is likely due to the overoxidation of the electrosynthesized polymer on the surface of the fMWCNT/GCE film electrode. To ensure the proper electrochemical polymerization of melamine, radical cations must be formed upon the oxidation of the monomer during the potential cycling to result in radical coupling.

Second, the peak-to-peak potential separation (ΔE_{pp}) of the final (20th) potential cycling is observed to be wider as the switching potentials increase from 1.4 to 1.6 V

Research article
doi.org/10.1002/elsa.202100021
Chemistry Europe
European Chemical Societies Publishing

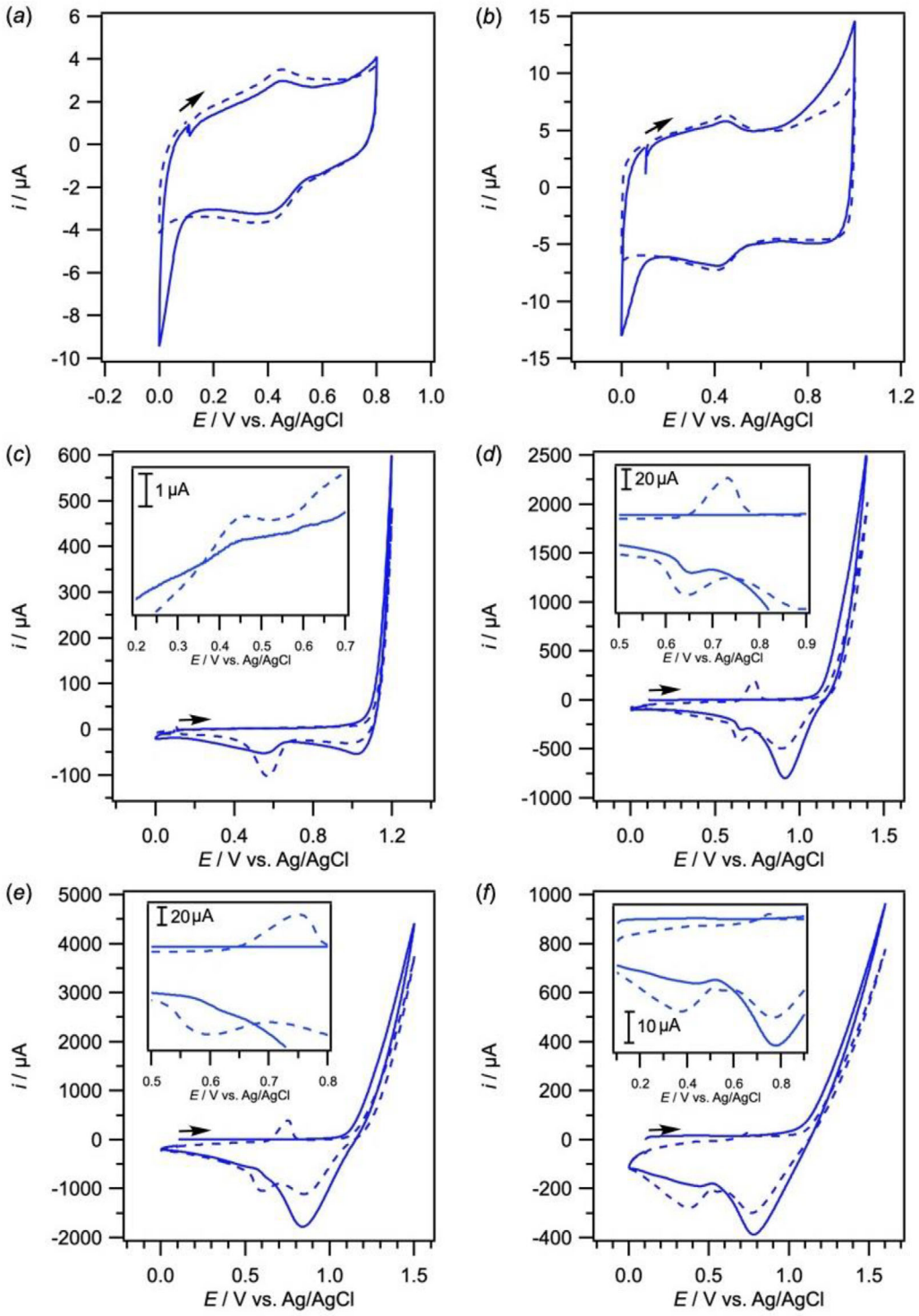

FIGURE 1 CVs for the electrochemical polymerization of 2 mM melamine on the surface of a 3-mm diameter fMWCNT/GCE film electrode in 1.0 M HCl solution at a scan rate of 20 mV/s for 20 cycles at 22 (±2)°C. Switching potentials: (a) 0.8 V, (b) 1.0 V, (c) 1.2 V, (d) 1.4 V, (e) 1.5 V and (f) 1.6 V. The solid (––) and dashed (- -) lines represent the 1st and 20th cycle of the potential cycling, respectively

(Figure 1d to f). The increasing trend is characteristic of increasingly sluggish electron transfer kinetics on the timescale of the potential sweep.

Third, there is a pronounced reduction wave in the range of 0.8 to 1.0 V when the scan is reversed at 1.4, 1.5, or 1.6 V resulting from the initial oxidation reaction of the water/electrolyte. The switching potentials (1.4 to 1.6 V) used in the experiments are approximately 0.2 to 0.4 V more than the theoretical decomposition potential of acidic water (+1.23 V).[23] Hence, the preferred

Research article
doi.org/10.1002/elsa.202100021
Chemistry Europe
European Chemical Societies Publishing

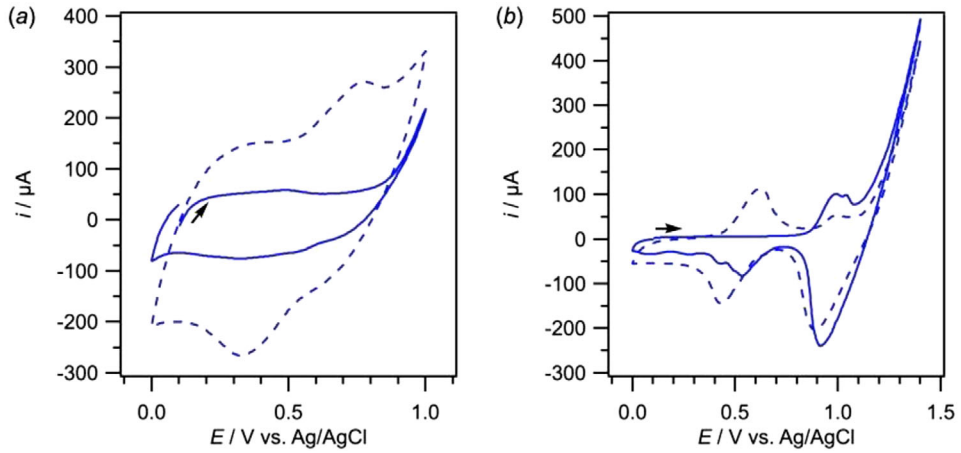

FIGURE 2 CVs for the electrochemical polymerization of 2 mM aniline on the surface of a 3-mm diameter fMWCNT/GCE film electrode in 1.0 M HCl solution with a scan rate of 20 mV/s for 20 cycles at 22 (±2)°C. Switching potentials: (a) 1.0 V and (b) 1.4 V. The solid (––) and dashed (- -) lines represent the 1st and 20th cycle of the potential cycling, respectively

switching potential for the electrochemical polymerization of melamine is selected at the lower 1.4 V to minimize the competing water/electrolyte oxidation reaction that produces interference in the voltammetric response due to the polymerization.[20,22]

The electrochemical polymerization of aniline in 1.0 M HCl was also investigated in 1.0 M HCl as the supporting electrolyte. It was previously reported that the formation of a nonconductive nanosized layer with aniline oligomers could passivate the electrode during the initial electrochemical oxidation of aniline (anodic scan).[24] Indeed, CVs of the electrochemical polymerization of 2 mM aniline with switching potentials of 1.0 and 1.4 V in Figure 2 exhibit no oxidative waves at 0.55 V in their first potential cycle. Depassivation follows in the reverse (cathodic) scan due to the reduction of the poorly conducting oligomers to form conducting and charged surface confined radical cations.[24] The chloride anions of the electrolyte also serve as dopants with a main purpose of intercalation/deintercalation to facilitate charge transfer across the electrochemically polymerized PANI on the surface of the fMWCNT/GCE film electrode.

Although the CVs at both switching potentials reveal an increase in the current density of the redox peaks as the potential cycling progressed up to the 20th cycle, different electrochemical behaviors were noted with both switching potentials (Figure 2). A quasi-rectangular shape of the CV curve characteristic of a pseudocapacitive material was observed with a switching potential of 1.0 V. At a switching potential of 1.4 V, a Faradaic pseudocapacitance behavior is noted with a pair of redox peaks between 0.4 and 0.6 V. The peaks are believed to involve the intercalation and deintercalation of chloride anions to cause electrochemical charge transfer and storage at the electroactive sites of the charged PANI radical species during the course of electrochemical polymerization. Hence, the switching potential of the voltammetric cycling was set at 1.4 V in order to facilitate the electrochemical copolymerization of aniline and melamine.

3.2 | Electrochemical copolymerization of both monomers

3.2.1 | Choice of monomeric ratio

In order to electrochemically copolymerize both melamine and aniline monomers onto the surface of the fMWCNT/GCE film electrode successfully, various monomeric concentration ratios were investigated. The CV in Figure 3 revealed that the ideal monomeric concentration ratio of aniline to melamine was 1:3 with 1.0 M HCl solution as the supporting electrolyte, so that the voltammetric peak heights for both polymers were the same. The green and red arrows at the respective redox peak potentials of both monomers in Figure 3 denote the increase in peak current upon successive potential cycling. At this monomeric ratio, the peak currents corresponding to the electrochemical polymerization of aniline and melamine are observed to be similar. When different monomeric ratios were examined, the peak current heights corresponding to melamine were much suppressed as compared to that of aniline. In other words, the extent of the electrochemical copolymerization is dependent on the concentration of melamine in the bulk solution. In addition, the oxidative peak potentials of aniline and melamine are noted at 0.55 and 0.71 V, respectively, while when the scan direction is reversed after first oxidizing the compounds, the cathodic peaks of aniline and melamine appear at 0.48 and 0.65 V,

Research article
doi.org/10.1002/elsa.202100021
Chemistry Europe
European Chemical Societies Publishing

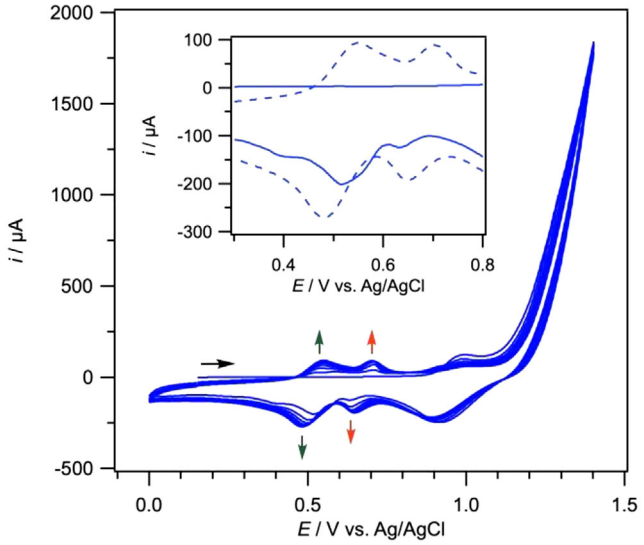

FIGURE 3 CVs for the electrochemical copolymerization of 1 mM aniline and 3 mM melamine monomers on the surface of a 3-mm diameter fMWCNT/GCE film electrode in 1.0 M HCl solution with a scan rate of 20 mV/s for eight cycles at 22 (±2)°C. Inset: The solid (––) and dashed (- -) lines represent the first and eight cycle of the potential cycling in zoom-in, respectively

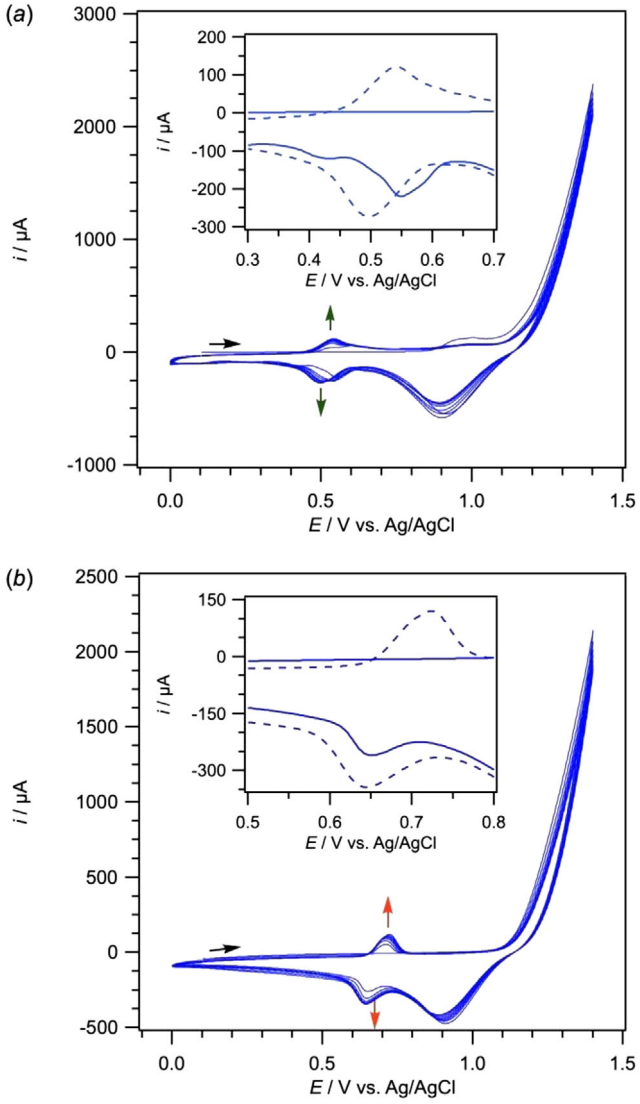

FIGURE 4 CVs for the electrochemical polymerization of (a) 1 mM aniline, and (b) 3 mM melamine monomers on the surface of a 3-mm diameter fMWCNT/GCE film electrode in 1.0 M HCl solution with a scan rate of 20 mV/s for eight cycles at 22 (±2)°C. Inset: The solid (––) and dashed (- -) lines represent the first and eight cycle of the potential cycling in zoom-in, respectively

respectively. The ΔE_{pp} values of the electrochemical copolymerization are then calculated to be 69 and 50 mV for aniline and melamine, respectively, which are consistent with a $2e^-/2H^+$ transfer process associated with both monomers.[22,25] In terms of the electrochemical behavior, the increase in peak currents and the potential shifts of the peaks during the electrochemical copolymerization with multiple scans (Figure 3) are largely similar with that observed for the electrochemical polymerization of the individual monomers (Figures 1 and 2) as described in Section 3.1.

In order to verify that the CV profile of the electrochemical copolymerization is similar with that of the individual electrochemical polymerization of each monomer, the latter was performed under similar experimental conditions with 1 mM aniline and 3 mM aniline in separate glass cells. The CVs recorded during the individual electrochemical polymerization of both monomers (Figure 4) reveal similar voltammetric profiles with that of the electrochemical copolymerization in terms of the redox peak potential values and the gradual increase in current heights with successive potential cycling. Therefore, we can confirm that there is electrochemical copolymerization onto the modified surface of the fMWCNT/GCE film electrode.

However, the current heights associated with the individual electrochemical polymerization of both monomers are higher than that of the electrochemical copolymerization. Such an observation is likely to be due to the competition for the electrochemical copolymerization of two monomers rather than the sole electrochemical polymerization of a monomer on an identical geometric electrode area. The presence of the fMWCNTs plays an important role during the electrochemical copolymerization by promoting noncovalent interactions with the copolymer species via π-π stacking, van der Waals, hydrogen bonding, and/or electrostatic interactions. The presence of the surface functional groups (–COOH) on the fMWCNTs promotes these interactions to occur during the electrochemical copolymerization of melamine and aniline in the presence of the acidic medium.[26] First, π-π stacking could occur between the fMWCNTs and the copolymers.[22] Hydrogen bonding can also occur between the –COOH

Research article
doi.org/10.1002/elsa.202100021
Chemistry Europe
European Chemical Societies Publishing

functional group of the fMWCNTs and the amine group of the copolymer species.[22,27] It is also important to note that these noncovalent interactions are more desired than the covalent interactions since the former does not cause modifications to the primary structure of the functionalized MWCNTs that can affect the voltammetric profile of the electrochemical copolymerization.[28]

3.2.2 | Choice of number of potential cycles

To control the degree of electrochemical copolymerization of aniline and melamine, the optimum number of successive potential cycles can be controlled by selecting the cycle number that results in the highest current density upon successive potential cycling in the monomer-containing electrolyte. The CVs recorded during the electrochemical copolymerization of aniline and melamine in a 1:3 monomeric ratio (Figure 3) revealed that eight potential cycles were the optimum number to register the maximum current heights associated with both monomers. Beyond the eight potential cycle, the current height of the daughter polymeric melamine did not increase and instead began to decrease very minimally. A slight increase in the composite film resistance could be the cause of the peak current decline that prevented further electron transfer. Repeats of the electrochemical copolymerization process under similar conditions reproduced the same result of eight potential cycles as the optimum number for potential cycling.

3.3 | Variable scan rates of the electrochemically copolymerized film electrode

The influence of variable scan rates on the electrochemical response of the electrochemically copolymerized PANIMEL/fMWCNT/GCE film electrode was investigated in a 1.0 M HCl solution in the absence of the monomers (after the initial coating procedure via performing eight CV scans). From Figure 5, the redox peak currents of the copolymerized film electrode were observed to increase with increasing scan rate.

In addition, the anodic and cathodic peak currents obtained from Figure 5a were found to be linearly related to the applied scan rate with the coefficient of determination (R^2) values of their linear regression equations very close to unity shown in Figure 6a. The following result, thus, entails a typical surface-confined electron transfer process that has occurred at the electrode-electrolyte interface, which is necessary for a high-specific capacitance of the modified electrode due to the pseudocapacitive properties of the CPs. Moreover, the result also confirmed that both

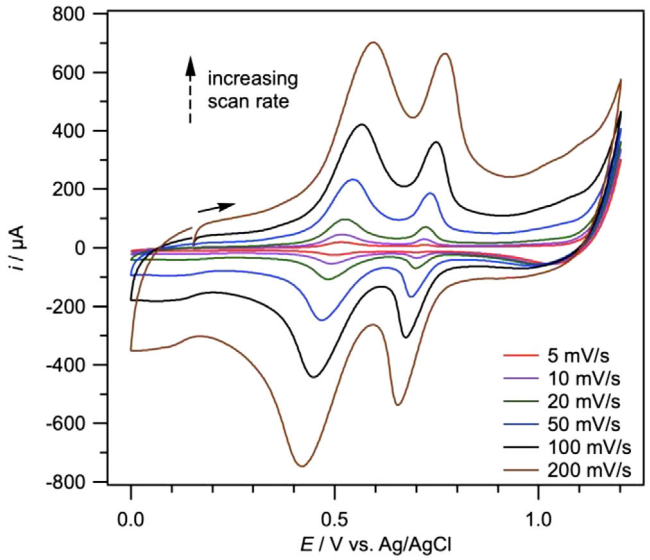

FIGURE 5 Scan rate dependent CVs of the 3-mm diameter PANIMEL/fMWCNT/GCE film electrode immersed in 1.0 M monomer-free HCl solution at 22 (±2)°C

aniline and melamine monomers were electrochemically copolymerized onto the surface of the fMWCNT/GCE film electrode. To further verify the dominance of a surface-confined electron transfer process, a linear plot of log anodic peak current ($i_p{}^{ox}$) versus log scan rate (v) is needed with its theoretical slope equal to a value of 1, while a dominant diffusion-controlled process is given by a slope value of 0.5.[29,30] From Figure 6b, the dependence of the $log\ i_p{}^{ox}$ on log v can be expressed by the following linear equations:

$$\log i_p{}^{ox} = 0.9653 \log v - 2.4198$$

for daughter polymeric aniline (dPANI)

$$\log i_p{}^{ox} = 1.1117 \log v - 2.3320$$

for daughter polymeric melamine (dMEL)

with their R^2 values of 0.9930 and 0.9905 corresponding to the daughter polymeric aniline and melamine, respectively. These linear equations have, thus, suggested that their slope values were approximately close to unity and confirmed that a dominant adsorption reaction has occurred during the electrochemical copolymerization process.

It was also observed that the separation between the oxidative to reductive peak potentials (ΔE_{pp}) of the daughter polymeric aniline and melamine shifted apart as the scan rate increased (Figure 6). Increasing the scan rate could result in poorer facilitation of the ion transport within the electrode interface, which results in lesser occupation of the active sites and pore structures in the electro-

Research article
doi.org/10.1002/elsa.202100021
Chemistry Europe
European Chemical Societies Publishing

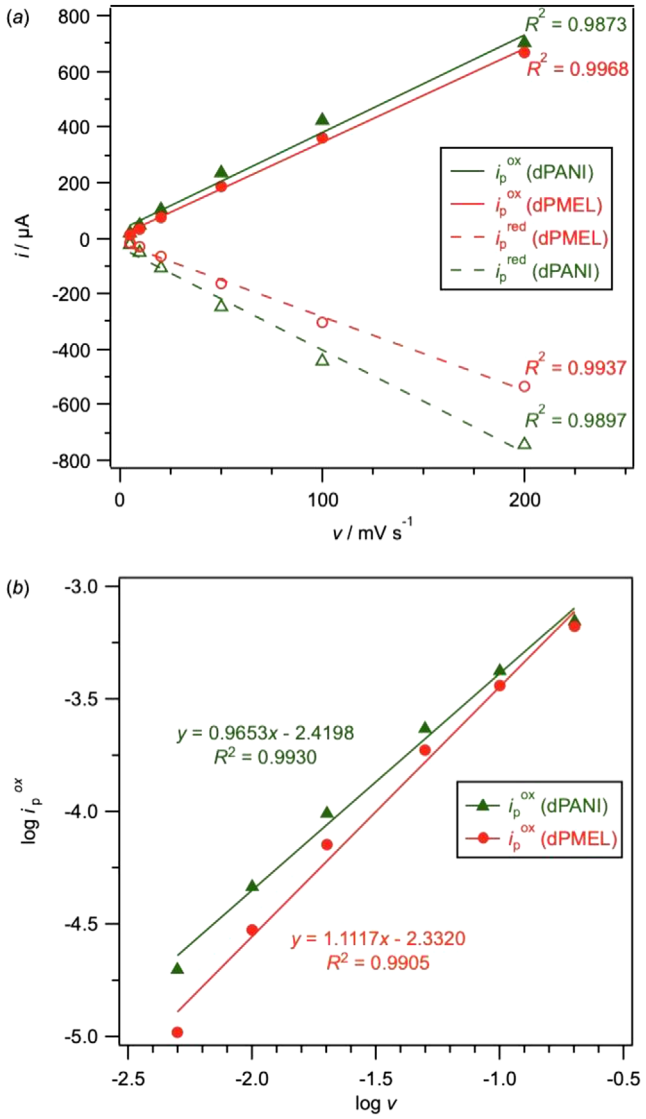

FIGURE 6 Linear plots of (a) peak current versus scan rate, and (b) log peak oxidative current versus log scan rate for the PANIMEL/fMWCNT/GCE film electrode immersed in 1.0 M monomer-free HCl solution at 22 (±2)°C

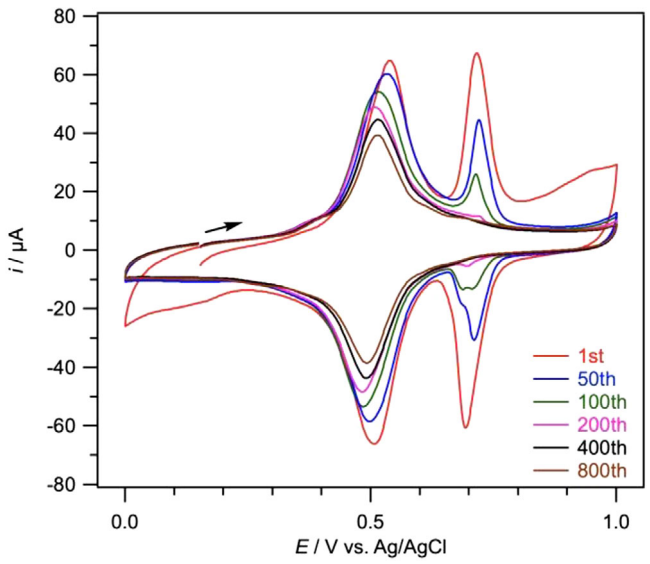

FIGURE 7 CVs of the 3-mm diameter PANIMEL/fMWCNT/GCE electrode immersed in 1.0 M monomer-free HCl solution with a scan rate of 20 mV/s at 22 (±2)°C. The legend depicts the particular cycle number of the stability test

chemically copolymerized film as well as a decrease in the heterogeneous electron transfer rate.

3.4 | Electrochemical stability of the electrochemically copolymerized film electrode

If the electrosynthesized film electrode exhibits poor cycling stability, its specific capacitance would be poor and result in a short cycle life. In order to investigate the electrochemical stability of the electrochemically copolymerized PANIMEL/fMWCNT/GCE film electrode, the newly electrosynthesized electrode was removed from the solution carefully and its surface rinsed with 1.0 M HCl to remove any monomer species. The electrode was subsequently transferred into a fresh 1.0 M HCl solution in the absence of the monomers to investigate the electrochemical stability of the electrochemically copolymerized film.

Figure 7 shows the CV recorded during the successive potential cycling of the PANIMEL/fMWCNT/GCE electrode in a monomer-free 1.0 M HCl solution. The decrease in the peak current characteristic of the daughters of the electrosynthesized copolymers can be explained with the possible loss of the active mass caused by the degradation of the electrochemical copolymerized film at the electrode-electrolyte interface.

Upon examination of Figure 7, the magnitude of the current densities related to the daughter polymeric melamine seems to decrease relatively faster than that related to the daughter polymeric aniline. Table 1 presents the cycle numbers related to the daughter polymeric monomers (aniline and melamine) which are determined graphically from Figure 7 at which the percentile of the anodic or cathodic peak current of the first potential cycling occurs. Indeed, the decrease in peak current was significantly much larger for the daughter polymeric melamine than the daughter polymeric aniline. The daughter polymeric monomers for aniline and melamine are observed to have 75% of their peak anodic currents occurring at the 211th and 38th potential cycle, respectively. The low potential cycle number with the daughter polymeric melamine is in contrast with supercapacitors having a virtually

TABLE 1 Cycle number related to the daughter polymeric monomers (aniline and melamine) at which the percentile of the anodic or cathodic peak current of the first potential cycling occurred

	Percentile of the anodic peak current (first potential cycling)		Percentile of the cathodic peak current (first potential cycling)	
	75%	50%	75%	50%
Cycle number related to the daughter polymeric aniline	211	>800	170	>800
Cycle number related to the daughter polymeric melamine	38	77	24	51

unlimited cycling life that is usually a minimum of 500,000 cycles. Hence, more work would need to be carried out on stabilizing the daughter polymeric melamine in order to mitigate the effect of large volumetric swelling-shrinkage behavior of the fMWCNT-CP composite caused by repetitive doping/dedoping with continuous cycling, and lead to an undesired poor capacitance.[31] Another reason for the poor cyclability could be due to the excessive nitrogen enrichment of the electrode film material that can lead to the properties of the film material such as conductivity, capacitance, and cyclability being compromised.[13] Poor porosity of the electrosynthesized film can also occur and lead to an apparently weak cycling stability of the polymeric melamine.[32,33] On the other hand, it cannot be ruled out that the bulk copolymer chains may have compromised the surface area of the fMWCNTs available for melamine to be electrochemically copolymerized on the modified electrode surface due to the head-to-head coupling as the only option for copolymerization. Hence, the electrolyte ions may not diffuse efficiently into the fMWCNT network and thereby limit the capacitance of the PANIMEL/fMWCNT/GCE film electrode.[34]

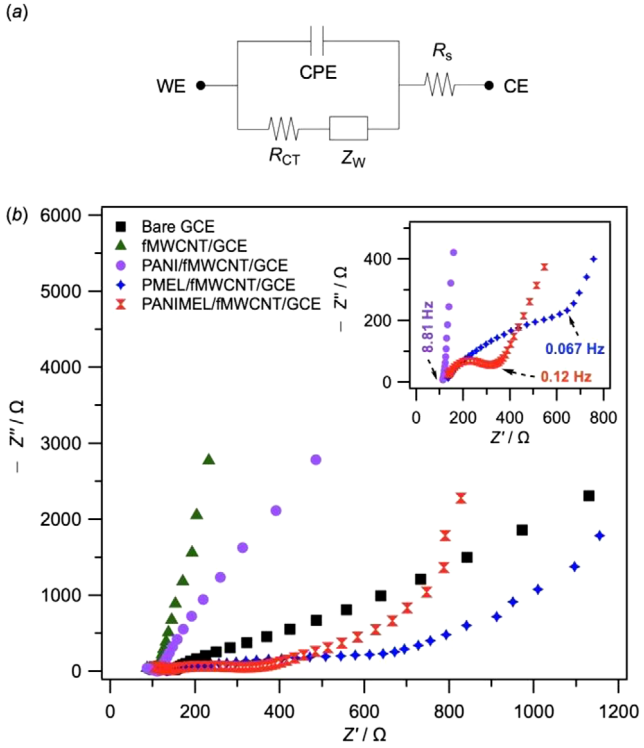

FIGURE 8 (a) The Randles equivalent circuit model used in the EIS measurements. (b) Nyquist plots of various electrodes immersed in 1.0 M HCl solution with 5 mM $[Fe(CN)_6]^{3-/4-}$ redox couple at 22 (±2)°C. Inset: Zoom-in of the Nyquist plots showing the three film electrodes PANI/fMWCNT/GCE, PMEL/fMWCNT/GCE and PANIMEL/fMWCNT/GCE and their knee frequency values

3.5 | Electrochemical impedance spectroscopy (EIS) of the various electrodes

In order to understand the interfacial properties of the electrode surfaces, EIS was performed with different electrodes in a three-electrode cell configuration. The frequency range used was within 0.1 to 60 kHz with the use of a redox probe of 5 mM $[Fe(CN)_6]^{3-/4-}$ and 1.0 M HCl as the supporting electrolyte. Figure 8a shows the Randles equivalent circuit model used in all EIS experiments of this study, whereby the solution resistance (R_S) is in series with the parallel connection of the constant phase element (CPE) and the charge transfer resistance (R_{ct}). In practice, the impedance of the electrosynthesized film electrodes deviates from the purely capacitive behavior and, thus, CPE was used in place of the single element C_{dl} (double layer capacitance). The EIS results are illustrated in the form of Nyquist plots in Figure 8b with the real Z' and imaginary Z'' components indicative of the ohmic and capacitive behaviors of the electrode, respectively.[35] The R_e, R_{ct}, specific capacitance C_{sp}, relaxation time constant τ, and phase angle θ were determined by fitting the impedance data with the use of the Randles equivalent circuit as summarized in Table 2.

The solution resistance (R_S) is given by the point of intersection with the real axis of the Nyquist plot at the high frequency region.[36] It is mainly caused by uncompensated solution resistance and the R_S values of the electrodes in Figure 8b are noted to be very close with each other.

Research article
doi.org/10.1002/elsa.202100021
Chemistry Europe
European Chemical Societies Publishing

TABLE 2 Impedance parameters of the various electrodes obtained from the fitting of the equivalent electric circuit to the experimental impedance data

Electrodes	$R_S/\Omega/cm^2$	$R_{ct}/\Omega/cm^2$	$C_{sp}/mF/cm^2$ [a]	$-\theta/°$ [b]
Bare GCE	13.37	115.20	0.08	62.2
fMWCNT/GCE	9.55	0.05	1.32	85.2
PANI/fMWCNT/GCE	10.00	2.05	0.68	75.0
PMEL/fMWCNT/GCE	12.04	97.42	6.29	57.2
PANIMEL/fMWCNT/GCE	12.20	17.10	4.94	70.0

[a]Areal capacitance values were determined at the lowest frequency of 0.05 Hz.
[b]Phase angles were determined from the Bode plot at the lowest frequency of 0.05 Hz.

By comparing the semicircle diameter of multiple Nyquist plots in Figure 8b, one can infer the extent of charge transfer resistance (R_{ct}) across all electrodes. The R_{ct} values of the various electrodes are observed to increase in the ascending order of fMWCNT/GCE < PANI/fMWCNT/GCE < PANIMEL/fMWCNT/GCE < PMEL/fMWCNT/GCE < bare GCE. A number of explanations could account for this observed trend. First, the semicircle of the fMWCNT/GCE film electrode is extremely small owing to the high porosity of the fMWCNT network that allows free diffusion of the electrolyte ions to the electrode surface. Second, surface-modified film electrodes have smaller R_{ct} values than the bare electrode, which highlights the importance of the porous fMWCNTs in facilitating charge transfer to the electrode surface and thereby lowering their R_{ct} values. Third, successive potential cycling could have resulted in a greater thickness of the polymeric film being electrodeposited on the electrode surfaces that are associated with the electrosynthesized film electrodes PANI/fMWCNT/GCE, PMEL/fMWCNT/GCE, and PANIMEL/fMWCNT/GCE. Consequentially, these three electrosynthesized film electrodes would have larger R_{ct} values than the fMWCNT/GCE film electrode. If these electrosynthesized film electrodes are compared with each other, the PANIMEL/fMWCNT/GCE copolymerized film electrode has a larger R_{ct} value than the PANI/fMWCNT/GCE film electrode, but smaller than that of the PMEL/fMWCNT/GCE film electrode. This observation is consistent with the result of the poor electrochemical stability of the daughter polymeric melamine discussed in Section 3.4. A poor ion insertion/deinsertion mechanism with the polymeric melamine species is then likely to cause a larger R_{ct} value associated with the PMEL/fMWCNT/GCE film electrode than the electrosynthesized copolymer film electrode. On the other hand, the presence of the more conductive and porous PANI species in the PANI/fMWCNT/GCE film electrode is believed to contribute a more efficient charge transfer than that in the electrosynthesized copolymer film electrode. Thus, the R_{ct} value of the PANI/fMWCNT/GCE film electrode is lower than that of the electrosynthesized copolymer film electrode followed by the PMEL/fMWCNT/GCE film electrode.

Figure 9 shows the corresponding Bode plots with the negative phase angles of these electrodes at the lowest frequency of 0.05 Hz in the ascending order of fMWCNT/GCE < PANI/fMWCNT/GCE < PANIMEL/fMWCNT/GCE < bare GCE < PMEL/fMWCNT/GCE. An ideal capacitor has a 90° negative phase angle characteristic of an EDLC while having a range from 65° to 80° in reality.[36] The phase angle values of the electrosynthesized fMWCNT/GCE, PMEL/fMWCNT/GCE and PANIMEL/fMWCNT/GCE film electrodes are close to the ideal value and also fall within the theoretical range suggesting good pseudocapacitive behavior.[37,38] One key observation is that the negative phase angles of both PANIMEL/fMWCNT/GCE and PANI/fMWCNT/GCE film electrodes were close with each other with only a small difference of 5°.

In general, the impedance of a device, Z is defined by Equation (1):

$$Z\ (\omega) = \frac{1}{j\omega C\ (\omega)} \tag{1}$$

where j is the unit imaginary number equal to the square root of –1, ω is the angular frequency with the mathematical expression $\omega = 2\pi f$, and C is the capacitance of the device. The areal (or specific) capacitance, C_{sp} of the electrode (Equation [2]) can be calculated by using the experimental data obtained from the Nyquist plots in Figure 8b:

$$C_{sp}\ (\omega) = \frac{1}{-Z''} \cdot \frac{1}{2\pi f A} \tag{2}$$

where $-Z''$ is the imaginary impedance, A is the surface area of electrode covered by active mass, and f is the frequency (in Hz) within the semicircle region of the Nyquist plot.[39,40] By comparing these electrodes with the use of a plot of areal capacitance as a function of frequency (in logarithmic scale) in Figure 9b, the PMEL/fMWCNT/GCE film electrode is noticed to have the highest C_{sp} value at high frequency among all of the electrodes. The C_{sp}

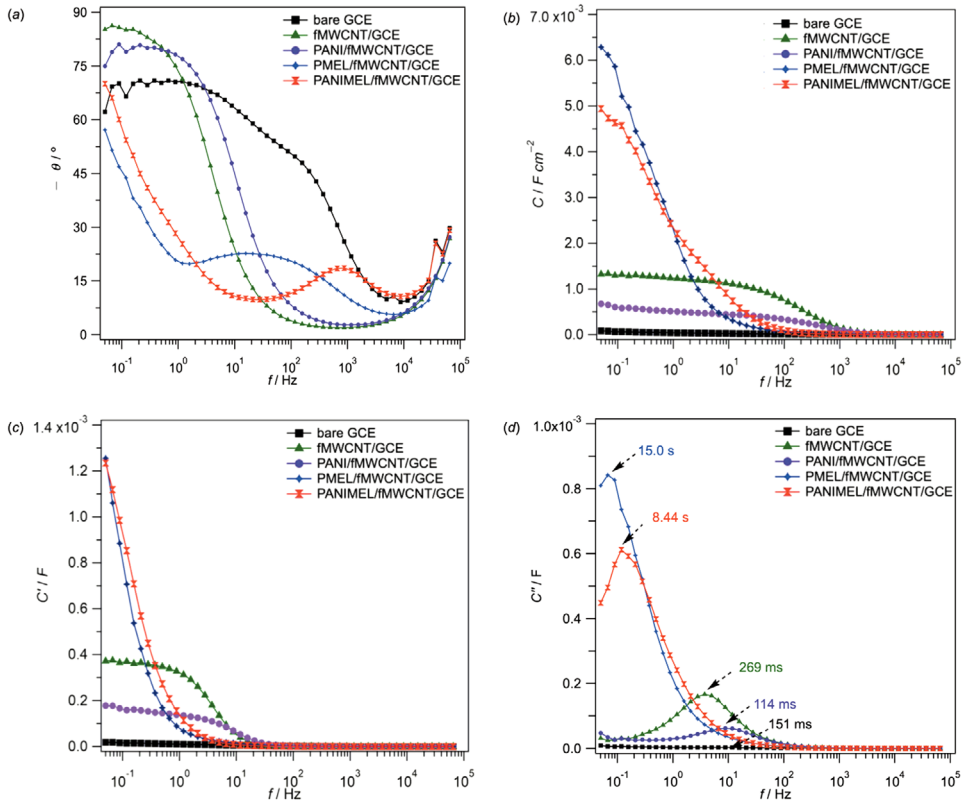

FIGURE 9 (a) Bode plots, (b) plots of areal capacitance (C_{sp}), (c) real capacitance (C'), and (d) imaginary capacitance (C'') of various electrodes as a function of frequency at 22 (±2)°C

values of the electrodes at high frequency follow the trend in an ascending order of PMEL/fMWCNT/GCE < PANIMEL/fMWCNT/GCE < PANI/fMWCNT/GCE < fMWCNT/GCE < bare GCE. Electrodes with film materials enriched in nitrogen have a significant impact on the electron donor-acceptor properties of the film material and the contribution of the heteroatom to the delocalized π-electron system.[13] With more nitrogen content, the C_{sp} value is expected to be greater.[41,14] However, there is competition for both aniline and melamine to be electrochemically copolymerized on the surface of the fMWCNT/GCE film electrode. Moreover, melamine has a much higher nitrogen content by mass than aniline. Thus, the C_{sp} value of the PANIMEL/fMWCNT/GCE copolymerized film electrode is observed to be lower than that of the PMEL/fMWCNT/GCE film electrode, but higher than that of the PANI/fMWCNT/GCE film electrode.

In practice, the device does not have perfect efficiency and energy losses must be accounted for. The capacitance, C of the device is the sum of its real and imaginary capacitances expressed by Equation (3):

$$C = C' - jC'' \tag{3}$$

where the real part C' relates to the effective capacitance that the device can deliver, while the imaginary part C'' accounts for the irreversible energy loss in the charge storage process. The real and imaginary capacitances are governed by Equations (4) and (5), respectively:

$$C'(\omega) = \frac{-Z''(\omega)}{\omega |Z(\omega)|^2} \tag{4}$$

$$C''(\omega) = \frac{Z'(\omega)}{\omega |Z(\omega)|^2} \tag{5}$$

where $Z'(\omega)$, $Z''(\omega)$ and $|Z(\omega)|$ are the real, imaginary and modulus impedances, respectively, as a function of angular frequency.[42] Using the experimental data obtained from the EIS measurements in Figure 8b, C' and C'' are then plotted separately against the frequency f (in logarithmic scale) as shown in Figure 9c and d. The latter plot is used to determine the relaxation time constant, τ of the device graphically as given by Equation (6):

$$\tau = \frac{1}{f_{max}} \tag{6}$$

Research article
doi.org/10.1002/elsa.202100021

TABLE 3 Values of the knee frequency and relaxation time constant for each electrode

Electrodes	f_{max}/Hz	τ/s
Bare GCE	6.61	0.15
fMWCNT/GCE	3.72	0.27
PANI/fMWCNT/GCE	8.80	0.11
PMEL/fMWCNT/GCE	0.067	15.0
PANIMEL/fMWCNT/GCE	0.118	8.44

where f_{max} is the knee frequency (in Hz) at which the device possesses negligible resistive behavior with maximum capacitance and energy dissipation. τ describes the rate capability of the electrode material and typically ranges from a few to tens of seconds with lower values favoring the higher power delivery of the device.[42,43] In addition, the electrode is ideally preferred with the lowest τ value coupled to a high f_{max} value in the Nyquist plot that is characteristic of a rapid discharge of the stored energy.[44] Figure 9d and Table 3 show that the PANIMEL/fMWCNT/GCE copolymerized film electrode (8.44 s) has a τ value smaller than the PMEL/fMWCNT/GCE film electrode (15.0 s), but 74 times greater than the PANI/fMWCNT/GCE film electrode (0.27 s). This result coincides well with the trend of R_{ct} and C_{sp} values observed in Figures 8b and 9b, respectively. In addition, it also reconfirms the likelihood of a greater diffusion resistance through the pores with a less efficient ion intercalation-deintercalation mechanism associated with the copolymerized film electrode than the PANI/fMWCNT/GCE film electrode.

3.6 | SEM and XPS analysis of the coated electrodes

The surface of the fMWCNT/GCE, PANI/fMWCNT/GCE, PMEL/fMWCNT/GCE, and PANIMEL/fMWCNT/GCE structures were examined using SEM and XPS. The SEM images appeared similar between the different coatings, which was to be expected as the surface morphology was determined by the drop-cast CNTs, which were the same for each structure (Figures S1-S4 in the Supporting Information). The XPS analysis provided support for the incorporation of PANI, and PMEL, and PANIMEL onto the CNTs through the identification of nitrogen peaks that were absent from the XPS analysis of the fMWCNT/GCE material (Figures S5-S8 in the Supporting Information). Furthermore, the PANI/fMWCNT/GCE and PANIMEL/fMWCNT/GCE materials also showed the presence of excess chloride that had entered the films as dopants to balance the positive charge during the polymerization process.

4 | CONCLUSIONS

A series of variables, including the electrode, switching potential, applied scan rate, and fMWCNTs, were investigated and evaluated during the individual electrochemical polymerization of aniline and melamine via successive potential cycling. The optimum monomeric ratio for the electrochemical copolymerization was subsequently determined as 1:3 aniline to melamine, respectively. Variable scan rate voltammetric studies of the electrosynthesized copolymer film electrode confirmed the dominance of the surface-confined electron transfer process at the electrode-electrolyte interface. The electrochemical stability of the copolymer film electrode was also assessed and demonstrated a limited cyclability of the daughter polymeric melamine, which was attributed to the excessive nitrogen content and low porosity with the daughter polymeric melamine that possibly led to a poor ion intercalation-deintercalation mechanism. ElS measurements were performed to study the interfacial properties of the electrode materials and compared with the control electrodes. Analysis of the EIS experimental data revealed that the copolymerized film electrode was electrochemically superior to the PMEL/fMWCNT/GCE film electrode but was inferior to the PANI/fMWCNT/GCE film electrode.

ACKNOWLEDGMENTS

The authors are grateful to the National Research Foundation (NRF) Singapore under its Campus for Research Excellence and Technological Enterprise (CREATE) program and the Singapore Government MOE Academic Research Fund Tier 1 Grant (RG3/19) for funding.

DATA AVAILABILITY STATEMENT

The data that support the findings of this study are available from the corresponding author upon reasonable request.

ORCID

Richard D. Webster https://orcid.org/0000-0002-0896-1960

REFERENCES

1. W. W. Clark, G. Cooke, *The Green Industrial Revolution: Energy, Engineering and Economics*, Elsevier, Amsterdams, Netherlands **2015**, p. 173–190.
2. D. N. Buckley, C. O'Dwyer, N. Quill, R. P. Lynch, in *Energy Storage Options and Their Environmental Impact* (Eds: R. E. Hester, R. M. Harrison), Royal Society of Chemistry Publishing, Cambridge, **2018**, p. 115–149.
3. A. Pandolfo, A. G. Hollenkamp, *J. Power Sources* **2006**, *157*, 11.
4. A. Eftekhari, L. Li, Y. Yang, *J. Power Sources* **2017**, *347*, 86.
5. M. F. L. De Volder, S. H. Tawfick, R. H. Baughman, A. J. Hart, *Science* **2013**, *339*, 535.

6. H. Wei, C. He, J. Liu, H. Gu, Y. Wang, X. Yan, J. Guo, D. Ding, N. Z. Shen, X. Wang, S. Wei, Z. Guo, *Polymer* **2015**, *67*, 192.
7. Z. Cao, B. Q. Wei, *Energy Environ. Sci.* **2013**, *6*, 3183.
8. K. Lota, V. Khomenko, E. Frackowiak, *J. Phys. Chem. Solids* **2004**, *65*, 295.
9. M. N. Hyder, S. W. Lee, F. Ç. Cebeci, D. J. Schmidt, Y. Shao-Horn, P. T. Hammond, *ACS Nano* **2011**, *5*, 8552.
10. F. Frackowiak, K. Jurewicz, S. Delpeux, F. Béguin, *J. Power Sources* **2001**, *97–98*, 822.
11. A. Godara, T. Vaugien, *JEC Compos.* **2009**, *46*, 64.
12. J. P. Paraknowitsch, A. Thomas, *Energy Environ. Sci.* **2013**, *6*, 2839.
13. G. Lota, K. Fic, E. Frackowiak, *Energy Environ. Sci.* **2011**, *4*, 1592.
14. E. Frackowiak, S. Depeux, K. Jurewicz, K. Szostak, D. Cazorla-Amoro, F. Béguin, *Chem. Phys. Lett.* **2002**, *361*, 35.
15. F. Béguin, V. Presser, A. Balducci, E. Frackowiak, *Adv. Mater.* **2014**, *26*, 2219.
16. V. Ruiz, C. Blanco, E. Raymundo-Piñero, V. Khomenko, F. Béguin, R. Santamaria, *Electrochim. Acta* **2007**, *52*, 4969.
17. S. I. Fletcher, F. B. Sillars, N. E. Hudson, P. J. Hall, *J. Chem. Eng. Data* **2010**, *55*, 778.
18. J.-C. Chiang, A. G. MacDiarmid, *Synth. Met.* **1986**, *13*, 193.
19. A. G. MacDiarmid, A. J. Epstein, *Faraday Discuss. Chem. Soc.* **1989**, *88*, 317.
20. S. Chen, S. Liu, A. Wen, J. Zhang, H. Nie, J. Chen, R. Zeng, Y. Long, Y. Jin, R. Mai, *Electrochim. Acta* **2018**, *271*, 312.
21. H. Wei, Y. Wang, J. Guo, X. Yan, R. O'Connor, X. Zhang, N. Z. Shen, B. L. Weeks, X. Huang, S. Wei, Z. Guo, *ChemElectroChem* **2015**, *2*, 119.
22. S. Baskar, C. W. Liao, J. L. Chang, J. M. Zen, *Electrochim. Acta* **2013**, *88*, 1.
23. M. P. Bichat, E. Raymundo-Piñero, F. Béguin, *Carbon* **2010**, *48*, 4351.
24. S.-Y. Hong, S.-M. Park, *J. Phys. Chem. B* **2007**, *111*, 9779.
25. I. Sapurina, A. V. Tenkovtsev, J. Stejskal, *Polym. Int.* **2015**, *64*, 453.
26. H. Fan, H. Wang, N. Zhao, X. Zhang, J. Xu, *J. Mater. Chem.* **2012**, *22*, 2774.
27. H. Wei, H. Gu, J. Guo, S. Wei, Z. Guo, *J. Electrochem. Soc.* **2013**, *160*, G3038.
28. K. Wu, S. Hu, *Carbon* **2004**, *42*, 3237.
29. A. M. Patil, A. C. Lokhande, P. A. Shinde, C. D. Lokhande, *ACS Appl. Mater. Interfaces* **2018**, *10*, 16636.
30. K. E. Ramohlola, G. R. Monana, M. J. Hato, K. D. Modibane, K. M. Molapo, M. Masikini, S. B. Mduli, E. I. Iwuoha, *Composites Part B* **2018**, *137*, 129.
31. S. R. Sivakkumar, J. M. Ko, D. Y. Kim, B. C. Kim, G. G. Wallace, *Electrochim. Acta* **2007**, *52*, 7377.
32. K. Jurewicz, K. Babeł, A. Źiółkowski, H. Wachowska, M. Kozłowski, *Fuel Process. Technol.* **2002**, *77–78*, 191.
33. K. Jurewicz, K. Babeł, A. Źiółkowski, H. Wachowska, *Electrochim. Acta* **2003**, *48*, 1491.
34. R. Malik, L. Zhang, C. McConnell, M. Scott, Y.-Y. Hsieh, R. Noga, N. T. Alvarez, V. Shanov, *Carbon* **2017**, *116*, 579.
35. A. Kumar, N. Kumar, Y. Sharma, J. Leu, T. Y. Tseng, *Nanoscale Res. Lett.* **2019**, *14*, 266.
36. A. S. ELmezayyen, S. Guan, F. M. Reicha, I. M. El-Sherbiny, J. Zheng, C. Xu, *J. Phys. D: Appl. Phys.* **2015**, *48*, 175502.
37. K. Krishnamoorthy, P. Pazhamalai, S. J. Kim, *Electrochim. Acta* **2017**, *227*, 85.
38. M. S. Kolathodi, M. Palei, T. S. Natarajan, *J. Mater. Chem. A* **2015**, *3*, 7513.
39. K. Chen, F. Liu, D. Xue, S. Komarneni, *Nanoscale* **2015**, *7*, 432.
40. A. Dettlaff, P. R. Das, L. Komsiyska, O. Osters, J. Łuczak, M. Wilamowska-Zawłocka, *Synth. Met.* **2018**, *244*, 80.
41. E. Frackowiak, *Phys. Chem. Chem. Phys.* **2007**, *9*, 1774.
42. C. Portet, P. L. Taberna, P. Simon, E. Flahaut, C. Laberty-Robert, *Electrochim. Acta* **2005**, *50*, 4174.
43. M. Lewandowski, M. Orzyłowski, *Bull. Pol. Ac.: Tech.* **2017**, *65*, 449.
44. A. Ghosh, V. T. Le, J. J. Bae, Y. H. Lee, *Sci. Rep.* **2013**, *3*, 2939.

SUPPORTING INFORMATION

Additional supporting information may be found online in the Supporting Information section at the end of the article.

How to cite this article: G. X. Tham, A. Subrata, A. C. Fisher, R. D. Webster, *Electrochem Sci Adv*. **2021**, e2100021.
https://doi.org/10.1002/elsa.202100021